0013-7227/05/$15.00/0
Printed in U.S.A.

Endocrinology 146(12):5086–5091

doi: 10.1210/en.2005-0063

Tau Is Hyperphosphorylated in the Insulin-Like Growth Factor-I Null Brain

Clara M. Cheng, Victor Tseng, Jie Wang, Daniel Wang, Ludmila Matyakhina, and Carolyn A. Bondy

Developmental Endocrinology Branch, National Institute of Child Health and Human Development, National Institutes of Health, Bethesda, Maryland 20892

IGF action has been implicated in the promotion of oxidative stress and aging in invertebrate and murine models. However, some *in vitro* models suggest that IGF-I specifically prevents neuronal oxidative damage. To investigate whether IGF-I promotes or retards brain aging, we evaluated signs of oxidative stress and neuropathological aging in brains from 400-d-old *Igf1*−/− and wild-type (WT) mice. Lipofuscin pigment accumulation reflects oxidative stress and aging, but we found no difference in lipofuscin deposition in *Igf1*−/− and WT brains. Likewise, there was no apparent difference in accumulation of nitrotyrosine residues in *Igf1*−/− and WT brains, except for layer IV/V of the cerebral cortex, where these proteins were about 20% higher in the *Igf1*−/− brain ($P = 0.03$). We found no difference in the levels of oxidative stress-related enzymes, neuronal nitric oxide synthase, inducible nitric oxide synthase, and superoxide dismutase in *Igf1*−/− and WT brains. Tau is a microtubule-associated protein that causes the formation of neurofibrillary tangles and senile plaques as it becomes hyperphosphorylated in the aging brain. Tau phosphorylation was dramatically increased on two specific residues, Ser-396 and Ser-202, both glycogen synthase kinases target sites implicated in neurodegeneration. These observations indicate that IGF-I has a major role in regulating tau phosphorylation in the aging brain, whereas its role in promoting or preventing oxidative stress remains uncertain. (*Endocrinology* 146: 5086–5091, 2005)

RECENT STUDIES IN *Caenorhabditis elegans* and mice have implicated the insulin/IGF system in reduced longevity and oxidative stress resistance (1, 2). Reduced expression of insulin, IGF-I, or downstream signaling molecules extend the life span significantly (1, 3–5). Also, mice heterozygous for IGF-I receptor gene deletion display increased resistance to oxidative stress and increased lifespan (6). However, IGF-I appears to protect neurons from oxidative stress *in vitro* (7–9). In addition, reduction in circulating and brain IGF-I levels have been associated with aging and neurodegenerative conditions, and IGF-I has been suggested as a therapeutic agent in amyotrophic lateral sclerosis and Alzheimer's disease (10–12). Thus, it has been suggested that increasing IGF-I may ameliorate the deterioration of brain aging and neurodegenerative disorders.

In this study, we used IGF-I gene-targeted mice (*Igf1*−/−) to investigate whether IGF-I promotes or retards brain aging. Age-related neurodegenerative disorders such as Alzheimer's and Parkinson's diseases are strongly correlated with oxidative stress. Hence, we examined biomarkers of oxidative damage, such as lipofuscin and nitrotyrosine residues in aged *Igf1*−/− and WT brains. Lipofuscin consists of intracellular autofluorescent pigments that are deposited in neuronal soma and processes during the aging process (13). The accumulation of nitrotyrosine residues is an indicator of the generation of reactive nitrogen species during aging progression. We also examined enzymes that regulate oxidative activity, such as superoxide dismutase (SOD) and nitric oxide synthase (NOS). SOD catalyzes the conversion of superoxide radicals to H_2O_2, which is converted to H_2O by peroxidase, protecting brain cells against oxidative stress (14). NOS, on the other hand, catalyzes synthesis of nitric oxide (NO), which then reacts with superoxide to form toxic peroxinitrite, causing cell damage during aging (15). In addition, brain aging is associated with increased phosphorylation of tau, a microtubule-associated protein involved in microtubule assembly and stabilization. Tau hyperphosphorylation is believed to lead to its disengagement from microtubule, destabilizing microtubule and disrupting normal microtubule-dependent processes (16). The unbound tau is thought to be more resistant to degradation and more prone to aggregation, culminating in the formation of neurofibrillary tangles (NFTs) (16, 17). Hyperphosphorylated, insoluble tau in the form of NFTs is associated with cognitive dysfunction in normal aging as well as a variety of late onset neurodegenerative disorders termed "tauopathies" (16, 18). We therefore evaluated tau protein levels and phosphorylation status in the aged *Igf1*−/− and WT control brains to elucidate IGF-I's role in regulation of this important neuropathological factor.

First Published Online August 25, 2005

Abbreviations: AD, Alzheimer's disease; GSK, glycogen synthase kinase; iNOS, inducible NOS; NFTs, neurofibrillary tangles; NOS, nitric oxide synthase; nNOS, neuronal NOS; PHF, paired helical filaments; SOD, superoxide dismutase; WT, wild type.

***Endocrinology* is published monthly by The Endocrine Society (http://www.endo-society.org), the foremost professional society serving the endocrine community.**

Materials and Methods

Animals

The mice used in this study were from an *Igf1* deletion line derived and genotyped as previously described (19). Animals were studied under protocols approved by the NICHD Animal Use and Care Committee. Male *Igf1*−/− mice and age-sex-matched littermates were euthanized at postnatal d 400 in CO_2 chamber followed by decapitation. Brains were rapidly dissected, cut along the sagittal midline, and snap frozen. One brain half was used for protein preparation, and the other

half was sectioned for histochemistry. Sections 10-μm thick were cut sagittally at −20 C, thaw-mounted onto poly-L-lysine-coated slides, and stored at −70 C until use.

Lipofuscin detection

Frozen sections were thawed and directly mounted with DAPI media (Vector Laboratories, Burlingame, CA). The sections were then examined directly under fluorescent microscope. The intracellular autofluorescent pigments known as lipofuscin gave a bright yellow fluorescent signal, whereas DAPI-stained nuclei gave a blue fluorescent signal. For the Sudan Black B staining, frozen sections were first fixed in 4% formaldehyde for 5 min, rinsed in water, and immersed in Sudan Black B reagent (Sigma Diagnostics, St. Louis, MO) overnight. After quick differentiation in 70% EtOH, the slides were washed in 50, 30% EtOH, water and then counterstained in Nuclear fast red (Sigma Diagnostics) for 3 min.

Immunohistochemistry

Immunohistochemistry was performed by the avidin-biotin-immunoperoxidase method (20). Briefly, frozen sections were fixed in 4% formaldehyde for 10 min then washed in 1× Tris/NaCl buffer [50 mM Tris/150 mM NaCl/0.1% Triton (pH 7.5)]. To remove endogenous peroxidase activity, slides were placed in 3% H_2O_2 solution for 10 min and then washed in the Tris/NaCl buffer. Nonspecific signal was blocked by incubating slides with 10% normal goat serum in blocking solution [1% BSA/0.02% Na-Azide/0.05% Triton X-100 in Tris/NaCl buffer (pH 7.5)] for 45 min. The sections were then incubated at 4 C with antinitrotyrosine antibody (1:500; Chemicon, Temecula, CA) overnight. After washing, the sections were incubated with biotinylated secondary antibodies (1:400; New England Biolabs, Beverly, MA) at room temperature for 40 min. The signal was amplified using the ABC peroxidase method (Vector Laboratories) and visualized with 3,3′-diaminibenzidine (Vector Laboratories). The semiquantitation of nitrotyrosine immunosignals was carried out in a blinded fashion. The signals were captured at ×200 using a video camera and analyzed using NIH image software (Image 1.57, NIH) in several brain structures, including frontal cortex layer II/III, layer VI/V, thalamus (ventrolateral thalamic nuclei and ventramedial thalamic nuclei), hypothalamus (lateral hypothalamus area) and striatum (accumbens nuclei). Background signal from each slide was subtracted before further analysis. Two sections from each brain were scored and n = 4 and 5 for *Igf1*−/− and WT controls, respectively. Differences between groups were compared by ANOVA followed by Fisher's least significant different tests.

Immunoblotting

Immunoblotting was performed according to Cheng *et al.* (21). Mouse brains (~0.4 g) were homogenized in a boiling solution containing 10 mM Tris (pH 7.4), 1 mM sodium orthovanadate, and 1% sodium dodecyl sulfate at a ratio of 1 g tissue to 17.5 ml solution. Ten microliters of each sample were loaded and resolved on NuPAGE 10% Bis-Tris Gels (Invitrogen Life Technologies, Carlsbad, CA) and transferred to nitrocellulose membranes using electrophoretic transfer cells (Bio-Rad, Hercules, CA). To ensure equal loading and transfer efficiency, the membranes were prestained with Ponceau S solution (Sigma) before immunodetection. Primary antibodies were purchased and diluted to use as follows: antiphospho-tau-396 (1:500; Zymed Laboratories, South San Francisco, CA), neuronal NOS (nNOS) and inducible NOS (iNOS) (1:1000; Chemicon International, Temecula, CA), SOD1 (1:500; Chemicon), tau-1 (1:500; Chemicon), AT-8 (1:100; Pierce Endogen, Rockford, IL), 12E8 (1:5000; provided by Dr. Peter Seubert at Elan Pharmaceuticals, Inc., San Francisco, CA) and tau-5 (1:500; Biosource International Inc., Camarillo, CA). After incubation with primary antibodies for 90 min and washed, the membranes were incubated with horseradish peroxidase-linked secondary antibodies for 60 min. Protein bands were then visualized using SuperSignal West Pico detection reagents (Pierce, Rockford, IL) on a Kodak image machine (Kodak, Rochester, NY). Digital image of the results from each blot was obtained, and the intensity of protein bands revealed by each specific antibody was compared and analyzed using Kodak 1D image-analysis software. Differences between groups were compared by ANOVA followed by Fisher's least significant different tests (n = 3–4 for *Igf1*−/− brains and n = 5 for WT controls). All the immunoblottings were repeated at least once, and the data were confirmed.

In situ hybridization

The tau clone (Image clone ID no. 746947, ATCC no. 1015357) was obtained from American Type Culture Collection (ATCC, Manassas, VA). This tau cDNA clone was sequenced and confirmed to contain the complete mouse tau coding region and partial 5′ and 3′ untranslated sequences. The cDNA clone was linearized with *Eco*RI for use as a template to synthesize antisense cRNA probe. The cRNA probe synthesis and *in situ* hybridization protocol were detailed previously (22). After hybridization, slides were exposed to Kodak Bio-Max MR film (Eastman Kodak, Rochester, NY) for 1 d and later dipped in Kodak NTB2 emulsion for 2 d. Parallel sections were hybridized to sense probes and processed together with antisense hybridization sections to serve as hybridization background control. Background signal from a sense probe was subtracted from raw data before further analysis. Film image was analyzed by NIH image program (Image 1.57, NIH). The quantitation of hybridization signal was carried out in a blinded fashion. Four measurements in each brain structure, including frontal cortex, thalamus and granule cell layer of cerebellum were taken for each animal to obtain group means. Hybridization signals on CA2 and CA3 of hippocampus were captured using a monochrome video camera under ×400 magnification and silver grains were counted with assistance of NIH image version 1.57 software. Statistical significance between two groups was compared by ANOVA followed by Fisher's least significant different tests (n = 4 for *Igf1*−/− brains and n = 5 for WT control).

Results

IGF-I null mice

The *Igf1*−/− mice have a very high perinatal mortality, largely due to hypoventilation (19). The mice that survive are dwarfs, reaching approximately 30–40% of WT size, depending on the strain (23). Whereas behavior is difficult to measure precisely in dwarfs, our study did not find any evidence for major neurological defects (20).

Lipofuscin

Accumulation of autofluorescent lipoprotein pigments (lipofuscin) in nerve cells is a typical feature of brain aging. Thus, we examined whether IGF-I deletion affected the lipofuscin deposition in aged brains by comparing sections from *Igf1* gene-deleted and age-matched WT mice. There were no apparent differences in the distribution or levels of autofluorescent signals in 400-d-old *Igf1*−/− brains compared with WT control brains (Fig. 1). This result was confirmed by lipid staining using Sudan Black B (data not shown).

Nitrotyrosine residues

To address whether IGF-I modulates brain oxidative stress, we investigated the deposition of nitrotyrosine residues (NT), the end-products of oxidative reactions. We found that NT distribution was similar in *Igf1*−/− and WT brains (Fig. 2). For example, NT immunostaining was apparent in Purkinje cells (Fig. 2, A and B) and in pyramidal neurons of the cerebral cortex (Fig. 2, C and D). The intensity of the immunostaining appeared similar in Purkinje cells, although they were markedly smaller in the *Igf1*−/− brain. Semiquantitation of immunostaining in cortical pyramids suggested a modest but significant increase in NT accumulation ($P = 0.03$) in cortical layer IV/V of *Igf1*−/− brains (Fig.

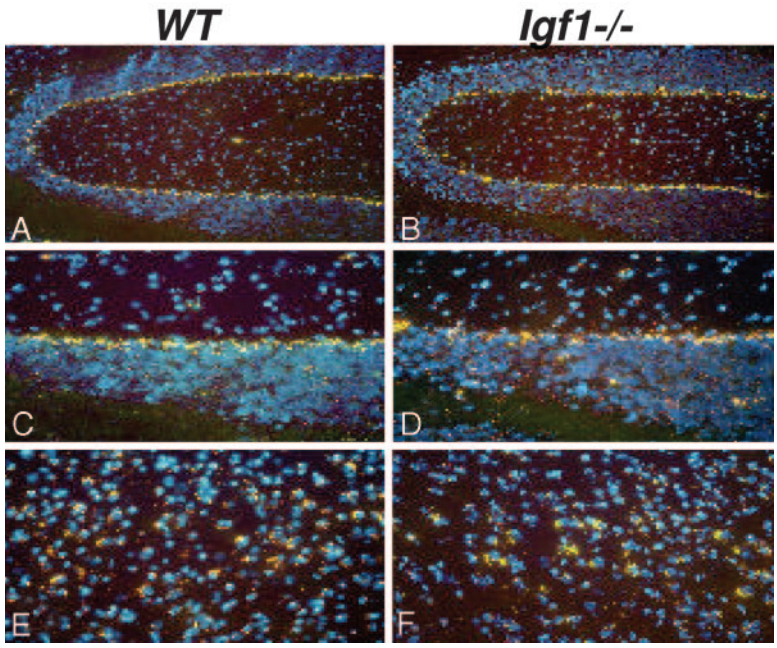

FIG. 1. Lipofuscin deposition in the aged *Igf1*−/− (B, D, and F) and WT (A, C, and E) brains. Fluorescent micrographs show similar lipofuscin deposition (*yellow*) in both *Igf1*−/− and WT brains. Nuclei are revealed by DAPI staining (*blue*). A–D, Representative micrographs showing lipofuscin fluorescence concentrated in Purkinje cells of the cerebellar cortex, with C and D at higher magnification. E and F, Lipofuscin in frontal cortex.

2E). However, NT levels were similar in *Igf1*−/− and WT brains in the thalamus, hypothalamus, striatum, and cerebellum (not shown).

Oxidation regulatory enzymes

We also evaluated enzymes involved in production of nitric oxide, nitric oxide synthetases (NOS) in these brains by immunoblotting (Fig. 3). We found similar levels of nNOS and iNOS in *Igf1*−/− and WT brains. There was a trend toward higher iNOS levels in *Igf1*−/− brains, but the difference between groups did not reach statistical significant (Fig. 3). SOD1 levels were also similar in *Igf1*−/− and WT brains (Fig. 3).

Tau

NFTs accumulate during brain aging as a result of increased phosphorylation of the microtubule-associated protein tau (17). To examine the effect of IGF-I deletion on tau phosphorylation in aged brains, we used Western blotting to evaluate the phosphorylation status of tau in *Igf1*−/− and WT brains. Anti-tau-396 antibodies recognize tau phosphorylated at serine 396, a site predominantly phosphorylated by GSK-3β (glycogen synthase kinase 3β) and prominent in pathological paired helical filaments (PHF) of neurofibrillary tangles (24). Tau phosphorylation at this specific epitope was increased by approximately 7-fold in the *Igf1*−/− brain compared with WT ($P = 0.004$) (Fig. 4). Another phospho-tau-specific antibody, AT-8, which recognizes PHF-associated tau, phosphorylated at serine 202, also detected a significant approximately 10-fold increased in *Igf1*−/− brain homogenate compared with WTs ($P = 0.02$). However, tau phosphorylation at serine 262 detected by 12E8 antibody showed no difference between *Igf1*−/− and WT brains. Total tau levels detected by the phospho-independent antibody, tau-5, were similar in *Igf1*−/− and WT brains (Fig. 4). Consistent with the above observations, the nonphosphorylated tau population, as detected by anti-tau-1 antibody (25, 26), was reduced in the *Igf1*−/− aged brains ($P < 0.01$). This result shows that tau is heavily phosphorylated on two serine sites in the brains of animals with IGF-I deficiency, suggesting that IGF-I normally prevents tau hyperphosphorylation at these specific sites.

To further investigate tau expression in *Igf1*−/− and WT mice, we performed *in situ* hybridization on anatomically matched brain sections. The anatomical distribution of tau mRNA was similar in *Igf1*−/− and WT mice (Fig. 5). Tau mRNA was concentrated in the dentate gyrus and Ammon's horn (Fig. 5, A and B) and in the granule cell layer as well as Purkinje cells of cerebellum (Fig. 5, C and D). Quantitative analyses in temporal cortex, thalamus, granule cell layer of cerebellum and CA2 and CA3 of hippocampus revealed that tau mRNA levels were similar in *Igf1*−/− and WT brains (data not shown).

Discussion

This study investigated the effects of IGF-I deletion on concomitants of brain aging, namely accumulation of oxidation by-products and tau phosphorylation. We found that aged *Igf1*−/− brains have similar levels of nitrotyrosine residues and lipofuscin deposition compared with WT brains. We found no difference in levels of enzymes involved in oxidative stress, such as NOS and SOD1, in *Igf1*−/− and WT control brains. These observations suggest that IGF-I normally has little effect on oxidative damage during brain aging. However, we found that the microtubule-associated protein tau is much more highly phosphorylated in the *Igf1* null brain, suggesting that IGF-I normally prevents tau hyperphosphorylation in the brain.

In healthy neurons, tau proteins regulate microtubule function in the nerve processes. Hyperphosphorylation dislodges tau from the microtubule surface, resulting in the accumulation of insoluble, toxic tau peptides and compro-

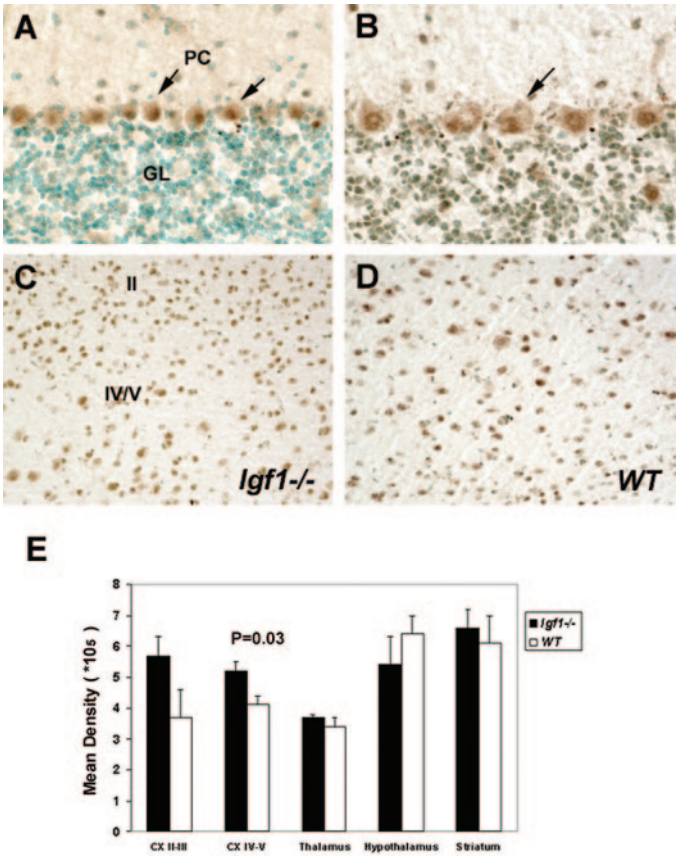

FIG. 2. Comparison of nitrotyrosine residue (NT) levels in the aged *Igf1*−/− and WT brains. Representative micrographs showed NT immunostaining concentrated in Purkinje cells (*arrows*) of the cerebellar cortex (A and B) and pyramidal neurons of the cerebral cortex (C and D) in *Igf1*−/− (A and C) and WT (B and D) brains. The cellular expression and distribution patterns of NT were similar in most brain regions. The results of semiquantitative analyses of the NT immunosignal in different brain regions are graphed in panel E.

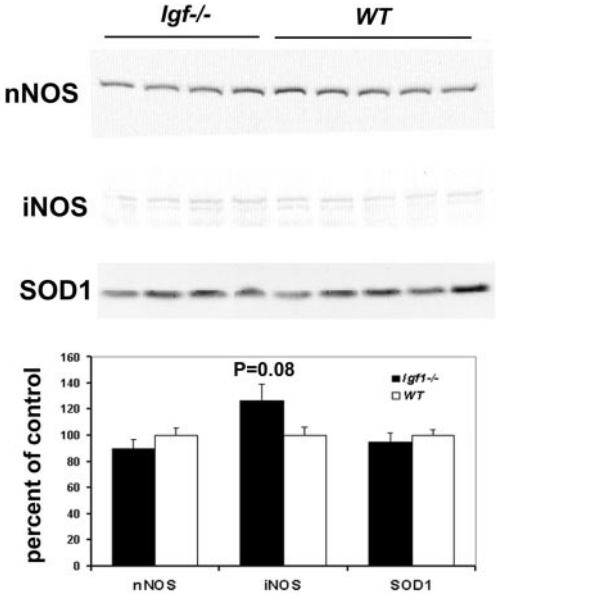

FIG. 3. NOS and SOD in aged *Igf1*−/− and WT brains. Immunoblotting analysis revealed no significant difference in the levels on nNOS or iNOS between aged *Igf1*−/− and WT brains, although iNOS levels were slightly higher in *Igf1*−/− brains, the difference did not reach statistical significance. Immunoblotting also revealed similar SOD1 levels in *Igf1*−/− and WT brains. Protein bands from the blots were quantified using computer-assistant image analysis. Data were expressed as mean ± SEM of percentage of WT values (n = 4 for *Igf1*−/− and n = 5 for WT brains).

mised axonal integrity (16, 17). In the brains of individuals with Alzheimer's disease (AD) and other neurodegenerative diseases, hyperphosphorylated tau is aggregated into intraneuronal deposits or NFTs (17). Analysis of tau protein from AD brains by mass spectrometry and sequencing revealed several persistently phosphorylated sites that are recognized by tau-directed antibodies, including tau-1 site (residues 191–225), carboxyl-terminal portion of the protein (residues 386–438) and Ser 262 (the numbering referred to the longest human tau isoform) (27, 28). In this report, we demonstrated the Ser-396, adjacent to microtubule-binding domain, and Ser-202, inside the tau-1 antibody binding site, are highly phosphorylated in the IGF-I null brain. Both sites are implicated in NFT formation. However, Ser-262 phosphorylation site was not altered by IGF-I deletion. Moreover, IGF-I deletion is not associated with reduced tau mRNA or protein levels. These observations suggest that IGF-I regulates tau phosphorylation on specific phosphorylation sites in the brain, but does not have a general effect on tau synthesis.

Tau-directed protein kinases may be divided into three groups: 1) second-messenger-activated kinases, including protein kinase C, protein kinase A, and $Ca2^{+}$/calmodulin-dependent kinase; 2) Ser/Pro-directed kinases, including MAPK, cyclin-dependent kinase 5, cell division cycle 2, GSK3α, GSK3β, and PAR-1 (29); and 3) other kinases, including $p110^{mapk}$ and casein kinase (for review see Ref. 30). These different kinases phosphorylate tau at various specific as well as overlapping sites (30), as for which kinases are most critical for AD-type NFT formation still under active debate. The present study illuminates the role of GSK3β in tau phosphorylation *in vivo* because IGF-I inhibits this kinase activity and specific GSK3β targets sites, Ser202 and Ser-396, are hyperphosphorylated in the IGF-I null brain. These GSK3β phosphoryated sites were well documented in *in vitro* studies (30–33). It is also well known that activation of IGF-I/insulin receptors triggers activation of the serine/threonine protein kinase Akt (34), which phosphorylates GSK-3β ser^{9}, resulting in its inhibition (35). We have previously shown that both GSK-3β and Akt phosphorylation are significantly reduced in the *Igf1* null brain compared with WT (36), suggesting that overactive GSK-3β may cause tau hyperphosphorylation in the *Igf1* null brain. All of these data indicate that disturbance in IGF-I signaling cascade leads to aberrant tau hyperphosphorylation, potentiating the formation of NFT.

GSK3β's contribution to tau-mediated neurodegeneration is unsettled; GSK3β overexpression was associated with tau hyperphosphorylation and neurodegeneration in some studies (37–39) but was associated with reduced neurodegeneration in a different murine model (40). This latter study in a complex, multiple transgenic model, found that although more hyperphosphorylated tau was present, neither an increase in insoluble tau aggregates nor the presence of paired helical filaments or tangles was observed. However, in hu-

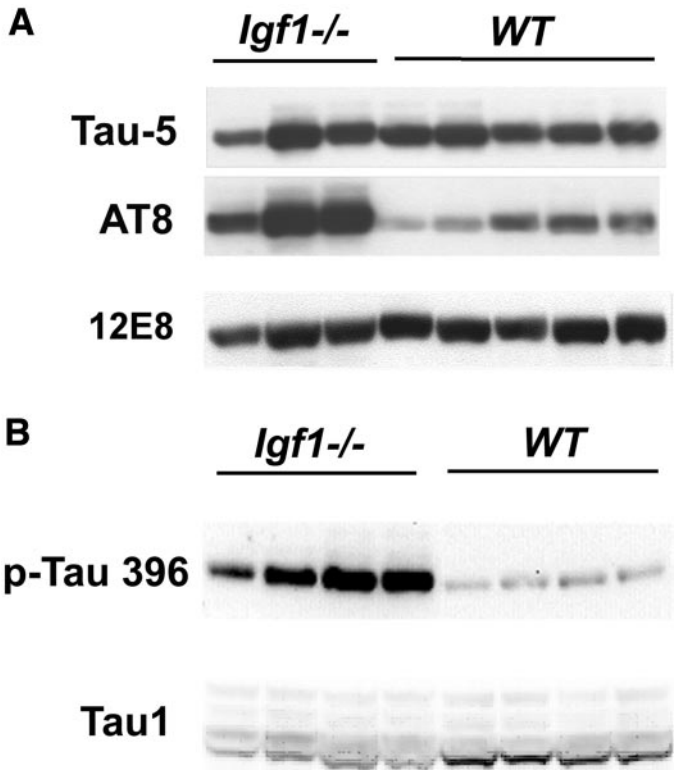

FIG. 4. Hyperphosphorylation of tau in the *Igf1*−/− brain. Total and phospho-tau immunoreactivity were examined in aged *Igf1*−/− and WT brains by immunoblots. A, Total tau was detected by anti-tau-5, which recognizes tau protein irrespective of its phosphorylation status. This exact blot was striped and reprobed with antibody AT-8 that recognizes PHF-tau with phosphorylated ser202 residue and later reprobed with antibody 12E8 that recognized phosphor-tau at ser 262. B, In another independent trial, phospho-tau was detected by antibody p-tau-396, that specifically recognizes tau phosphorylation on serine 396, a site prominently phosphorylated in PHF-tau. The same blot was then stripped and reprobed with tau-1 antibody, which detects dephosphorylated tau. These blots show that total tau protein is preserved in *Igf1*−/− brain, whereas tau phosphorylation is dramatically increased in aged *Igf1*−/− brains compared with WTs.

man brains NFTs invariably contain tau phosphorylated on GSK3β target sites and GSK3β is consistently found colocalized with pretangle and tangle-bearing neurons (41). The mouse brain does not normally exhibit the neuropathological hallmarks of human brain aging and neurodegenerative disorders such as amyloid plaques or NFTs (42), and we did not detect such abnormal markers in either *Igf1* null or WT brain in this study. However, the present study provides an important *in vivo* loss-of-function model illustrating a role for IGF-I in regulation of tau phosphorylation by inhibition of GSK3β, potentially impacting tau-mediated neurodegeneration in the mature/aging murine brain. This may be a somewhat more physiological model than previous studies based on GSK3β overexpression in cell culture or transgenic animals for its link to tau hyperphosphorylation (33, 37, 43).

This study found similar levels of SOD and NOS enzymes, and similar markers of oxidative damage in *Igf1*−/− and WT brains, except for a small increase in nitrotyrosine residues detected in cortical layer IV/V in the *Igf1*null mouse. This could mean that IGF-I does not normally have a major role in mature brain oxidative activity or antioxidant defenses.

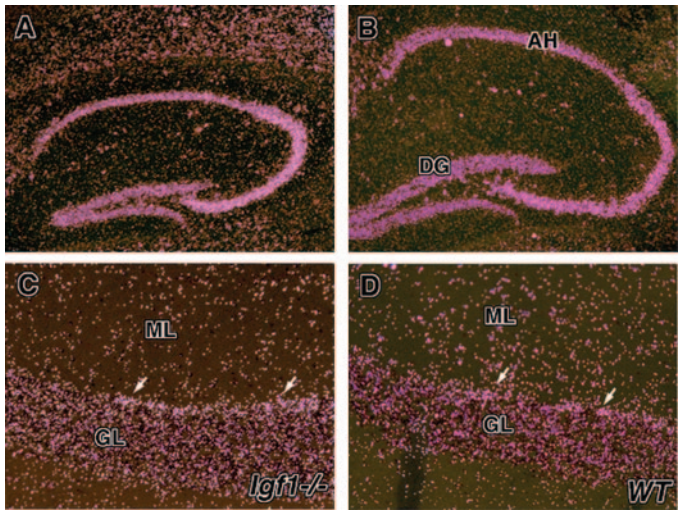

FIG. 5. Tau gene expression was examined by *in situ* hybridization in *Igf1*−/− (A and C) and WT aging brains (B and D). Representative dark-field micrographs show tau mRNA hybrid signal as *pink silver* grains concentrated in the dentate gyrus (DG) and Ammon's horn (AH) of hippocampal formation (A and B) and in the granule cell layer as well as Purkinje cells (*arrows*) of cerebellum (C and D). There was no apparent difference in brain tau mRNA levels between two groups.

However, lipofuscin and NT residues are relatively nonspecific markers of neuronal oxidative activity, and it remains possible that IGF-I is active in specific metabolic pathways we have not detected with this methodology.

IGF-I and/or insulin have been implicated in other aspects of neurodegenerative disease (12, 44). The human brain affected by Alzheimer-type deterioration is consistently found to exhibit reduced glucose use (45, 46). We have previously shown a highly significant positive correlation between local IGF-I expression and brain glucose use in the maturing mouse brain (36), suggesting that reduction in local or perhaps circulating IGF-I levels may contribute to reduced glucose metabolism and cerebral dysfunction in the adult. Recently, a potential relation between reduced insulin/IGF-I signaling and β-amyloid accumulation has also been suggested (46, 47). Therefore, reduced IGF-I/insulin signaling is implicated in several major pathological features of AD, including amyloidosis, NFT, cell demise and aberrant brain glucose use. These observations suggest that preventing the age-related decline in circulating (48) and brain IGF-I levels (49, 50) may help reduce the risk of AD.

Acknowledgments

We thank Dr. Shu-Hui Yen at Mayo Clinic for discussion in tau pathologies and Dr. Peter Seubert at Elan Pharmaceuticals, Inc. (San Francisco, CA) for providing the 12E8 antibody.

Received January 18, 2005. Accepted August 15, 2005.

Address all correspondence and requests for reprints to: Clara Cheng, Building 10/CRC 1-3330, 10 Center Drive, National Institutes of Health, Bethesda, Maryland 20892. E-mail: chengc@mail.nih.gov.

References

1. **Clancy DJ, Gems D, Harshman LG, Oldham S, Stocker H, Hafen E, Leevers SJ, Partridge L** 2001 Extension of life-span by loss of CHICO, a Drosophila insulin receptor substrate protein. Science 292:104–106

2. **Wolkow CA, Kimura KD, Lee MS, Ruvkun G** 2000 Regulation of *C. elegans* life-span by insulinlike signaling in the nervous system. Science 290:147–150
3. **Brown-Borg HM, Borg KE, Meliska CJ, Bartke A** 1996 Dwarf mice and the ageing process. Nature 384:33
4. **Kenyon C, Chang J, Gensch E, Rudner A, Tabtiang R** 1993 A *C. elegans* mutant that lives twice as long as wild type. Nature 366:461–464
5. **Tatar M, Kopelman A, Epstein D, Tu MP, Yin CM, Garofalo RS** 2001 A mutant Drosophila insulin receptor homolog that extends life-span and impairs neuroendocrine function. Science 292:107–110
6. **Holzenberger M, Dupont J, Ducos B, Leneuve P, Geloen A, Even PC, Cervera P, Le Bouc Y** 2003 IGF-1 receptor regulates lifespan and resistance to oxidative stress in mice. Nature 421:182–187
7. **Russell JW, Sullivan KA, Windebank AJ, Herrmann DN, Feldman EL** 1999 Neurons undergo apoptosis in animal and cell culture models of diabetes. Neurobiol Dis 6:347–363
8. **Heck S, Lezoualc'h F, Engert S, Behl C** 1999 Insulin-like growth factor-1-mediated neuroprotection against oxidative stress is associated with activation of nuclear factor κB. J Biol Chem 274:9828–9835
9. **Gustafsson H, Soderdahl T, Jonsson G, Bratteng JO, Forsby A** 2004 Insulin-like growth factor type 1 prevents hyperglycemia-induced uncoupling protein 3 down-regulation and oxidative stress. J Neurosci Res 77:285–291
10. **Kaspar BK, Llado J, Sherkat N, Rothstein JD, Gage FH** 2003 Retrograde viral delivery of IGF-1 prolongs survival in a mouse ALS model. Science 301:839–842
11. **Gasparini L, Xu H** 2003 Potential roles of insulin and IGF-1 in Alzheimer's disease. Trends Neurosci 26:404–406
12. **Trejo JL, Carro E, Garcia-Galloway E, Torres-Aleman I** 2004 Role of insulin-like growth factor I signaling in neurodegenerative diseases. J Mol Med 82: 156–162
13. **Terman A, Brunk UT** 1998 Lipofuscin: mechanisms of formation and increase with age. APMIS 106:265–276
14. **Fridovich I** 1995 Superoxide radical and superoxide dismutases. Annu Rev Biochem 64:97–112
15. **Beckman JS, Koppenol WH** 1996 Nitric oxide, superoxide, and peroxynitrite: the good, the bad, and ugly. Am J Physiol 271:C1424–C1437
16. **Lee VM, Goedert M, Trojanowski JQ** 2001 Neurodegenerative tauopathies. Annu Rev Neurosci 24:1121–1159
17. **Spillantini MG, Goedert M** 1998 Tau protein pathology in neurodegenerative diseases. Trends Neurosci 21:428–433
18. **Geschwind DH** 2003 Tau phosphorylation, tangles, and neurodegeneration: the chicken or the egg? Neuron 40:457–460
19. **Powell-Braxton L, Hollingshead P, Warburton C, Dowd M, Pitts-Meek S, Dalton D, Gillett N, Stewart TA** 1993 IGF-I is required for normal embryonic growth in mice. Genes Dev 7:2609–2617
20. **Cheng CM, Joncas G, Reinhardt RR, Farrer R, Quarles R, Janssen J, McDonald MP, Crawley JN, Powell-Braxton L, Bondy CA** 1998 Biochemical and morphometric analyses show that myelination in the insulin-like growth factor 1 null brain is proportionate to its neuronal composition. J Neurosci 18:5673–5681
21. **Cheng CM, Mervis RF, Niu SL, Salem Jr N, Witters LA, Tseng V, Reinhardt R, Bondy CA** 2003 Insulin-like growth factor 1 is essential for normal dendritic growth. J Neurosci Res 73:1–9
22. **Zhou J, Chin E, Bondy C** 1991 Cellular pattern of insulin-like growth factor-I (IGF-I) and IGF-I receptor gene expression in the developing and mature ovarian follicle. Endocrinology 129:3281–3288
23. **Wang J, Zhou J, Powell-Braxton L, Bondy C** 1999 Effects of Igf1 gene deletion on postnatal growth patterns. Endocrinology 140:3391–3394
24. **Hoffmann R, Lee VM, Leight S, Varga I, Otvos Jr L** 1997 Unique Alzheimer's disease paired helical filament specific epitopes involve double phosphorylation at specific sites. Biochemistry 36:8114–8124
25. **Binder LI, Frankfurter A, Rebhun LI** 1985 The distribution of tau in the mammalian central nervous system. J Cell Biol 101:1371–1378
26. **Biernat J, Mandelkow EM, Schroter C, Lichtenberg-Kraag B, Steiner B, Berling B, Meyer H, Mercken M, Vandermeeren A, Goedert M, Mandelkow E** 1992 The switch of tau protein to an Alzheimer-like state includes the phosphorylation of two serine-proline motifs upstream of the microtubule binding region. EMBO J 11:1593–1597
27. **Hasegawa M, Morishima-Kawashima M, Takio K, Suzuki M, Titani K, Ihara Y** 1992 Protein sequence and mass spectrometric analyses of tau in the Alzheimer's disease brain. J Biol Chem 267:17047–17054
28. **Morishima-Kawashima M, Hasegawa M, Takio K, Suzuki M, Yoshida H, Watanabe A, Titani K, Ihara Y** 1995 Hyperphosphorylation of tau in PHF. Neurobiol Aging 16:365–371
29. **Nishimura I, Yang Y, Lu B** 2004 PAR-1 kinase plays an initiator role in a temporally ordered phosphorylation process that confers tau toxicity in Drosophila. Cell 116:671–682
30. **Billingsley ML, Kincaid RL** 1997 Regulated phosphorylation and dephosphorylation of tau protein: effects on microtubule interaction, intracellular trafficking and neurodegeneration. Biochem J 323(Pt 3):577–591
31. **Imahori K, Uchida T** 1997 Physiology and pathology of tau protein kinases in relation to Alzheimer's disease. J Biochem (Tokyo) 121:179–188
32. **Takashima A, Honda T, Yasutake K, Michel G, Murayama O, Murayama M, Ishiguro K, Yamaguchi H** 1998 Activation of tau protein kinase I/glycogen synthase kinase-3β by amyloid β peptide (25–35) enhances phosphorylation of tau in hippocampal neurons. Neurosci Res 31:317–323
33. **Michel G, Mercken M, Murayama M, Noguchi K, Ishiguro K, Imahori K, Takashima A** 1998 Characterization of tau phosphorylation in glycogen synthase kinase-3β and cyclin dependent kinase-5 activator (p23) transfected cells. Biochim Biophys Acta 1380:177–182
34. **Summers SA, Birnbaum MJ** 1997 A role for the serine/threonine kinase, Akt, in insulin-stimulated glucose uptake. Biochem Soc Trans 25:981–988
35. **Cross DA, Alessi DR, Cohen P, Andjelkovich M, Hemmings BA** 1995 Inhibition of glycogen synthase kinase-3 by insulin mediated by protein kinase B. Nature 378:785–789
36. **Cheng CM, Reinhardt RR, Lee WH, Joncas G, Patel SC, Bondy CA** 2000 Insulin-like growth factor 1 regulates developing brain glucose metabolism. Proc Natl Acad Sci USA 97:10236–10241
37. **Lucas JJ, Hernandez F, Gomez-Ramos P, Moran MA, Hen R, Avila J** 2001 Decreased nuclear β-catenin, tau hyperphosphorylation and neurodegeneration in GSK-3β conditional transgenic mice. EMBO J 20:27–39
38. **Hernandez F, Borrell J, Guaza C, Avila J, Lucas JJ** 2002 Spatial learning deficit in transgenic mice that conditionally over-express GSK-3β in the brain but do not form tau filaments. J Neurochem 83:1529–1533
39. **Li B, Ryder J, Su Y, Moore Jr SA, Liu F, Solenberg P, Brune K, Fox N, Ni B, Liu R, Zhou Y** 2004 Overexpression of GSK3βS9A resulted in tau hyperphosphorylation and morphology reminiscent of pretangle-like neurons in the brain of PDGSK3β transgenic mice. Transgenic Res 13:385–396
40. **Spittaels K, Van den Haute C, Van Dorpe J, Geerts H, Mercken M, Bruynseels K, Lasrado R, Vandezande K, Laenen I, Boon T, Van Lint J, Vandenheede J, Moechars D, Loos R, Van Leuven F** 2000 Glycogen synthase kinase-3β phosphorylates protein tau and rescues the axonopathy in the central nervous system of human four-repeat tau transgenic mice. J Biol Chem 275:41340–41349
41. **Pei J-J, Braak E, Braak H, Iqbal K, Winblad B, Cowburn RF** 1999 Distribution of active glycogen synthase kinase 3β (GSK-3β) in brains staged for Alzheimer disease neurofibrillary changes. J Neuropathol Exp Neurol 58:1010–1019
42. **Gotz J, Streffer JR, David D, Schild A, Hoerndli F, Pennanen L, Kurosinski P, Chen F** 2004 Transgenic animal models of Alzheimer's disease and related disorders: histopathology, behavior and therapy. Mol Psychiatry 9:664–683
43. **Hong M, Lee VM-Y** 1997 Insulin and insulin-like growth factor-1 regulate tau phosphorylation in cultured human neurons. J Biol Chem 272:19547–19553
44. **van Dam PS, Aleman A** 2004 Insulin-like growth factor-I, cognition and brain aging. Eur J Pharmacol 490:87–95
45. **Silverman DH, Small GW, Chang CY, Lu CS, Kung De Aburto MA, Chen W, Czernin J, Rapoport SI, Pietrini P, Alexander GE, Schapiro MB, Jagust WJ, Hoffman JM, Welsh-Bohmer KA, Alavi A, Clark CM, Salmon E, de Leon MJ, Mielke R, Cummings JL, Kowell AP, Gambhir SS, Hoh CK, Phelps ME** 2001 Positron emission tomography in evaluation of dementia: regional brain metabolism and long-term outcome. JAMA 286:2120–2127
46. **Hoyer S** 2004 Glucose metabolism and insulin receptor signal transduction in Alzheimer disease. Eur J Pharmacol 490:115–125
47. **Carro E, Torres-Aleman I** 2004 The role of insulin and insulin-like growth factor I in the molecular and cellular mechanisms underlying the pathology of Alzheimer's disease. Eur J Pharmacol 490:127–133
48. **Breese CR, Ingram RL, Sonntag WE** 1991 Influence of age and long-term dietary restriction on plasma insulin-like growth factor-1 (IGF-1), IGF-1 gene expression, and IGF-1 binding proteins. J Gerontol 46:B180–B187
49. **Lai M, Hibberd CJ, Gluckman PD, Seckl JR** 2000 Reduced expression of insulin-like growth factor 1 messenger RNA in the hippocampus of aged rats. Neurosci Lett 288:66–70
50. **Sonntag WE, Lynch CD, Bennett SA, Khan AS, Thornton PL, Cooney PT, Ingram RL, McShane T, Brunso-Bechtold JK** 1999 Alterations in insulin-like growth factor-1 gene and protein expression and type 1 insulin-like growth factor receptors in the brains of ageing rats. Neuroscience 88:269–279

Endocrinology **is published monthly by The Endocrine Society (http://www.endo-society.org), the foremost professional society serving the endocrine community.**